Water isotope ratio (d2H and d18O) measurements in atmospheric moisture using an optical feedback cavity enhanced absorption laser spectrometer

Rosario Iannone, D. Romanini, Olivier Cattani, Harro A.J. Meijer, E. R. T. Kerstel

HAL Id: hal-00563780

https://hal.science/hal-00563780

Submitted on 7 Feb 2011

1 Water isotope ratio (δ^2H and δ^{18}O) measurements in atmospheric
2 moisture using an optical feedback cavity enhanced
3 absorption laser spectrometer

4 Rosario Q. Iannone,[1] Daniele Romanini,[2] Olivier Cattani,[3] Harro A. J. Meijer,[1]
5 and Erik R. Th. Kerstel[1]

7 [1] Water vapor isotopes represent an innovative and excellent tool for understanding
8 complex mechanisms in the atmospheric water cycle over different time scales, and they
9 can be used for a variety of applications in the fields of paleoclimatology, hydrology,
10 oceanography, and ecology. We use an ultrasensitive near-infrared spectrometer,
11 originally designed for use on airborne platforms in the upper troposphere and lower
12 stratosphere, to measure the water deuterium and oxygen-18 isotope ratios *in situ*, in
13 ground-level tropospheric moisture, with a high temporal resolution (from 300 s down to
14 less than 1 s). We present some examples of continuous monitoring of near-surface
15 atmospheric moisture, demonstrating that our infrared laser spectrometer could be used
16 successfully to record high-concentration atmospheric water vapor mixing ratios in
17 continuous time series, with a data coverage of ~90%, interrupted only for daily calibration
18 to two isotope ratio mass spectrometry–calibrated local water standards. The
19 atmospheric data show that the water vapor isotopic composition exhibits a high variability
20 that can be related to weather conditions, especially to changes in relative humidity.
21 Besides, the results suggest that observed spatial and temporal variations of the stable
22 isotope content of atmospheric water vapor are strongly related to water vapor transport in
23 the atmosphere.

27 1. Introduction

28 [2] To obtain detailed knowledge of the hydrological
29 cycle, information on all three phases of water is required.
30 Isotopic analysis of atmospheric trace gases provides a
31 valuable tool for resolving their budgets because the phys-
32 ical, chemical, or biological processes involved fractionate
33 isotopically in unique ways and leave characteristic isotopic
34 signatures in the trace gas. In particular, water vapor iso-
35 topes provide information concerning the mechanisms of
36 processes that occur in the water cycle, such as evaporation
37 at the surface of the Earth and subsequent transport and
38 phase changes in the atmosphere.

39 [3] The Global Network for Isotopes in Precipitation
40 (GNIP), founded in 1958 by the World Meteorological
41 Organization and the International Atomic Energy Agency
42 (IAEA), has been surveying the isotopic composition of

43 precipitation water since 1961 [*Araguas Araguas et al.*,
44 1996]. The network consists of about 100 sampling sites
45 around the world, including marine, coastal, and inland sta-
46 tions. Through those measurements, some information has
47 already been obtained about the isotopic composition of
48 atmospheric moisture, assuming that application of the
49 Rayleigh condensation model is valid: the isotope distribu-
50 tion in precipitation is an "equilibrium proxy" for the one in
51 the vapor phase. This assumption is based on the concept of
52 temperature-dependent equilibrium isotope exchange effects.
53 However, because precipitation predominantly occurs as
54 discrete events in both space and time, sampling of liquid
55 water does not provide an estimate of vapor isotopic com-
56 position with high temporal resolution, and it does not pro-
57 vide information on changes occurring between precipitation
58 events, or in areas with low or even zero precipitation. This
59 has motivated new efforts to obtain more data on the spatial
60 and temporal variation in the isotopic composition of
61 atmospheric moisture.

62 [4] A second network was thus initiated by the IAEA in
63 1994. This network was named Moisture Isotopes in the
64 Biosphere and Atmosphere and it is intended to complement
65 and expand the GNIP (http://www-naweb.iaea.org/napc/ih/
66 MIBA/IHS_MIBA_current.html).

[1]Centrum voor IsotopenOnderzoek, University of Groningen, Groningen, Netherlands.
[2]Laboratoire de Spectrométrie Physique, UMR 5588, Université J. Fourier Grenoble, CNRS, Saint Martin d'Hères, France.
[3]LSCE, IPSL CEA Saclay, Gif sur Yvette, France.

[5] Water-vapor isotope measurements can be used to reveal a possible relationship between water-vapor isotopes and ambient moisture. In addition, atmospheric humidity shows a diurnal pattern and it would be interesting to verify the existence of this variation in the isotopes signal. Ultimately, the information obtained in these atmospheric moisture isotope studies can be used to improve the representation of processes such as evaporation and condensation in climatic simulations.

[6] Isotopic variations in H_2O vapor are usually reported as delta values, expressed in per mil (‰), giving the deviation of the ratio of the rare isotope to the most abundant isotope, relative to a standard. The internationally accepted standard material, used in hydrological applications, is known as Vienna standard mean ocean water (VSMOW) [Gonfiantini, 1978]. If we define R to be the ratio $[^2H]/[^1H]$ or $[^{18}O]/[^{16}O]$ in the sample or in the standard, we thus have

$$\delta = \left[\frac{R_{sample} - R_{standard}}{R_{standard}} \right]. \tag{1}$$

Although the determination of the isotopic content of rainfall is a fairly straightforward process, measuring isotopic ratios in the vapor is not easily performed and requires sophisticated equipment.

[7] The conventional technique for this specific application generally involves the use of cold traps cooled to roughly $-80°C$ in order to collect water vapor, followed by laboratory isotope ratio mass spectrometry (IRMS) analyses. Jacob and Sonntag [1991] recorded almost continuous time series (sampling period of 1 or 2 days) of δ^2H and $\delta^{18}O$ in atmospheric water vapor at Heidelberg (Germany) over a time span of 8 years. We also cite the effort of He and Smith [1999], who sampled water vapor from a light aircraft above a forest in New England, Connecticut (United States), and Wang and Yakir [2000], who measured water-vapor stable isotopes to study evapotranspiration fluxes above canopies.

[8] Another option is to measure the water-vapor isotopic distributions from space using a satellite-based spectrometer. Worden et al. [2007] used the Tropospheric Emission Spectrometer on board the Aura spacecraft to obtain a characterization of the vertical profiles of $^1H^{16}O^2H$ and $H_2^{16}O$ in the tropical region. It is worth noting that both cryogenic whole air sampling and satellite remote sensing produce measurements with limited temporal resolution, spatial resolution, or both.

[9] Optical spectroscopy enables long time series of onsite measurements with high temporal coverage. Lee et al. [2005] carried out continuous measurements of $H_2^{18}O/H_2^{16}O$ in atmospheric water vapor in New Haven, Connecticut (United States), using a commercial Campbell-Scientific tunable diode laser (TDL) gas analyzer. Later, Wen et al. [2008], extended this study to include measurements of δ^2H using an upgraded version of the TDL analyzer. Griffith et al. [2006] used a Fourier transform infrared (FTIR) spectrometer to perform measurements of δ^2H in an Australian eucalypt forest near Tumbarumba, New South Wales, in southeastern Australia. Both these works describe systems for measurement of atmospheric water vapor isotopes in real time, based on infrared spectroscopy. Both the Campbell Scientific and the FTIR instruments are fairly big and require liquid nitrogen cooling for laser and/or detector operation.

[10] Finally, very recently, measurements of δ^2H and $\delta^{18}O$ of atmospheric moisture were carried out by Wang et al. [2009], whose aim was to calibrate an off-axis integrated cavity output spectrometer, manufactured by Los Gatos Research, Inc. (http://www.lgrinc.com). The precisions achieved with this instrument were ~0.1‰ for ^{18}O and 0.4‰ for ^2H, for an averaging time of over 500 s. Continuous records of isotopic composition of water vapor were also reported by Galewsky et al. [2009], who performed in situ measurements at the Mauna Loa Laboratory in Hawaii. They used three laser spectrometers, of which two were commercial (Los Gatos Research, Inc., and Picarro, Inc., http://www.picarro.com), whereas the third laser-based spectrometer was developed at the Jet Propulsion Laboratory.

[11] Here we demonstrate that the infrared laser spectrometer we previously developed for airborne applications [Kerstel et al., 2006; Iannone et al., 2009b] can be successfully applied to the isotopic characterization (δ^2H and $\delta^{18}O$) of atmospheric, near-surface moisture through real-time and continuous measurements with an accuracy and precision comparable to that of cryogenic sampling and IRMS, but with a much higher temporal resolution. The instrument is lightweight (3 kg for the optical core, excluding the computer and pump) and small (~25 L), has a low power consumption (~150 W), and requires no liquid nitrogen, making it ideally suited for field operation. It has a large dynamic range of absorption measurement, a feature in common with the commercial Los Gatos Research and Picarro near-infrared water vapor isotope ratio spectrometers. In addition, all three spectrometers are able to operate autonomously, and the small size and the high degree of portability make the analyzers easily transportable to the field for use in in situ measurements.

[12] In the Los Gatos Research analyzer, the incoherent coupling to a very dense cavity mode structure produces a very low level of output signal compared to the other two techniques and, consequently, requires a fairly high laser power and a good signal detection system. Moreover, the optical cell necessarily incorporates very large diameter mirrors, which makes the gas cell volume large, and thus increases the pumping requirement, if the gas exchange time (which limits the instrument response time) must be kept short. Our spectrometer and the Picarro analyzer share the advantage of a very small cavity volume. An advantage of the particular technique used in our spectrometer is the inherent frequency calibration of the spectrum. For this purpose, the Picarro analyzer is equipped with a proprietary wavelength monitor module, which adds complexity and cost to the instrument. Calibration of the (relative) frequency scale is important in that it is a prerequisite for very precise model fits to the spectral absorption features, which generally improve the long-term reproducibility of the absorption measurements.

[13] We show preliminary measurements of water-vapor isotope ratios in ambient air, sampled at the rooftop of the Center for Isotope Research in Groningen, Netherlands (53° 13′N, 6°33′E) during two 1-week measurement campaigns, when the instrument was not needed within its designated project of airborne isotope ratio analysis of atmospheric moisture. Although the spectrometer performance was

below its optimum (the noise equivalent absorption, NEA, was almost a factor of 3 worse than what can be obtained with the same setup and some sample introduction issues were identified, as is discussed farther down), we use the data here to show the wealth of information that can be obtained with online continuous monitoring of atmospheric, and thus relatively high water content, moisture, which does not require the utmost sensitivity of the instrument. We demonstrate that the results substantially surpass a conventional offline cryogenic sampling strategy in terms of information content.

2. Methods

2.1. Experimental Setup

[14] In recent years, several laser spectroscopic methods have been proposed, developed, and optimized for isotopic investigations, especially in the infrared region [*Kerstel*, 2004; *Kerstel and Gianfrani*, 2008]. In this region, most molecular species exhibit strong vibrational-rotational absorption bands. This feature, combined with the use of diode lasers, enables the resolution of single spectral lines of a molecule and to discriminate between different isotopologues.

[15] The instrument used here was designed and constructed to use near-infrared diode laser absorption spectroscopy to detect water vapor isotopologues with a room temperature, distributed feedback laser (Laser Components GmbH) operating around 1.39 μm (7184 cm^{-1}). The laser is tuned over a 1 cm^{-1} spectral range, enabling the nearly simultaneous registration of H$_2$O isotopologue spectral features, including rovibrational absorption lines belonging to H^{16}OH, H^{17}OH, H^{18}OH, and ^{1}HO^{2}H. The δ^{17}O measurements are not considered here since they do not, and in fact are not expected to, yield information beyond that provided by δ^{18}O because of the relationship between ^{17}O and ^{18}O observed in all tropospheric meteoric waters [*Meijer and Li*, 1998]. In order to see deviations from this behavior in tropospheric, evaporated water, extremely high precision measurements of δ^{17}O and δ^{18}O are required, which are beyond the capabilities of this spectrometer [*Barkan and Luz*, 2007].

[16] The device uses the sensitive technique of optical feedback cavity enhanced absorption spectroscopy (OFCEAS) and was developed in collaboration with the University of Grenoble. Advantages of OFCEAS, compared to other laser spectroscopic techniques, include the large dynamic range, enabling isotope ratio measurements over almost three orders of magnitude in the water-vapor mixing ratio, and a small gas cell volume, enabling a fast gas exchange and spectrometer response. For a detailed description of the experimental apparatus we refer to a previous publication [*Kerstel et al.*, 2006], whereas its principle of operation is described by *Morville et al.* [2005].

[17] The technique of CEAS yields a direct measurement of the wavelength-dependent absorption coefficient a, which can be written as the product of the number density n, the normalized line shape function f, the line strength S, and the absorption path length l:

$$a(\nu) = n(p,T)f(p,T,\nu-\nu_0)S(T)l, \qquad (2)$$

where p and T represent the total pressure and temperature of the sample in the spectrometer cavity, ν represents the laser frequency, and ν_0 represents the line-center frequency. Integration of the absorption coefficient over the entire line profile f (i.e., the "line area") directly yields the number density of the associated species, assuming the line strength is known. The line strengths of the absorption lines used in this study, as well as their temperature and pressure dependencies, are all tabulated in the HITRAN database [*Rothman et al.*, 2005]. The effective path length is determined by frequent calibration of the absorbance scale of the spectrometer by means of cavity ring down measurements [*Kerstel et al.*, 2006].

[18] The mixing ratio is calculated assuming ideal gas behavior. The isotope ratios, instead, are given by the super-ratio of the absorption coefficients of the rare and abundant isotopologues in the sample and a reference material [*Kerstel*, 2004] and, thus, require no knowledge of the line strengths. For example, in the case of oxygen-18,

$$\delta^{18}\text{O} = \frac{\left[a(\text{H}^{18}\text{OH})/a(\text{H}^{16}\text{OH})\right]_{\text{sample}}}{\left[a(\text{H}^{18}\text{OH})/a(\text{H}^{16}\text{OH})\right]_{\text{reference}}} - 1. \qquad (3)$$

We note that equation (3) differs from equation (1) in the use of molecular instead of atomic quantities. It can be shown that the molecular isotopologue abundance ratios, ^{2}R$_M$ = [HO^{2}H]/2[H$_2$O] for deuterium and $^{17/18}$R$_M$ = [H$_2^{17/18}$O]/[H$_2^{16}$O] for oxygen-17/18, are in good approximation equal to their atomic counterparts (such as ^{2}R = [^{2}H]/[^{1}H]). This equivalence of molecular and atomic values is an even better approximation for the case of the "delta value" ($\delta = R_{\text{sample}}/R_{\text{reference}} - 1$) of equation (3) [*Kerstel*, 2004].

[19] The reference ratio of the absorption coefficients is determined experimentally through periodic calibration measurements on local standard materials that are well characterized on the international, two-point VSMOW-SLAP (standard light Antarctic precipitation) isotope scale [*Gonfiantini*, 1984; *Hut*, 1987], as explained in more detail in section 2.2.

[20] The whole setup is housed in an insulated aluminum case, thermally regulated by two ribbon heaters (MINCO) to a temperature of 32°C. To facilitate thermal exchange, two ventilators are placed inside the box. A flow is established inside the gas cell by means of a molecular drag pump. The flow rate is adjusted via a manual valve, while the gas pressure inside the cell is stabilized independently of the flow by a forward pressure controller (Bronkhorst). The pressure is therefore kept stable at a value of 40 mbar. The small gas cell volume of ~20 mL ensures a fast gas cell exchange (<4 s) with a very modest pumping speed of 150 mL/min (Alcaltel Drytel 1025) [*Kerstel et al.*, 2006].

2.2. Calibration System

[21] Figure 1 represents a schematic of the gas handling system used to calibrate the measurement of the atmospheric water isotopes. The gas flow system basically has three operational modes: ambient air inlet and either one of two calibration gas streams. Outside ambient air was continuously drawn through the system by means of fused silica-coated (1/4-in. OD) tubing (O'Brien) leading from the rooftop of our laboratory (line 3). As the flow inside the
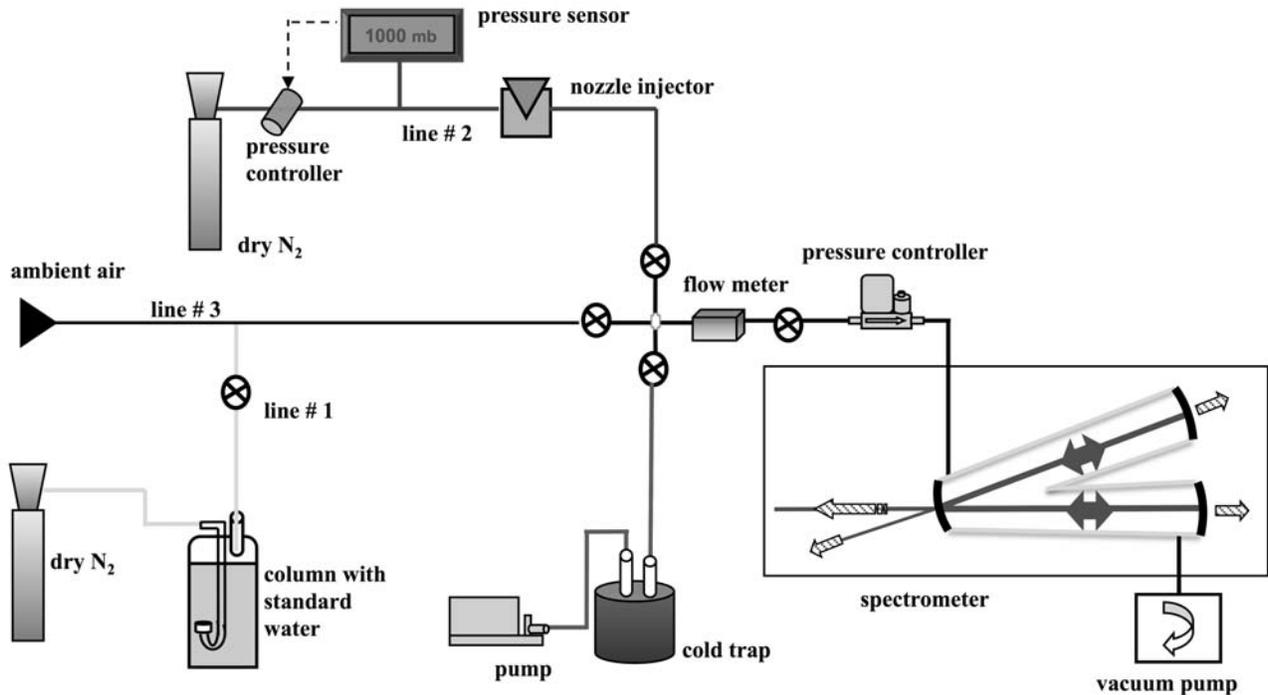
Figure 1. Sketch of the experimental arrangement used to calibrate the atmospheric measurements of water vapor isotope ratios. Three gas lines were used, one to lead atmospheric air to the laser spectrometer (line 3), and the other two for delivery of reference water vapor (lines 1 and 2), as explained in the text (section 2.2). The pressure controller establishes a pressure of 40 mbar inside the optical cell, whereas the flow was regulated to 150 mL/min by a metering valve at the exit of the spectrometer.

298 tube remains laminar, the length of the tube (10 m) does not
299 noticeably alter the overall system response time, which
300 was demonstrated to be 2 s in a series of measurements
301 carried out by switching between synthetic air and labora-
302 tory air. A 50 μm nylon filter was inserted at the beginning
303 of the sampling line in order to eliminate particles from the
304 airstream.

305 [22] The atmospheric measurements were interrupted
306 once or twice daily for calibration measurements using two
307 local isotopic standard waters. The use of two reference
308 waters enables the calibration of the atmospheric moisture
309 measurements to a two-point isotope scale in a procedure
310 similar to the standard VSMOW-SLAP calibration proce-
311 dure described by *Gonfiantini* [1984] and *Hut* [1987].

312 [23] Two calibration lines were installed. In the case of
313 tropospheric water vapor characterized by a mixing ratio
314 higher than 5000 ppmv, as encountered during measure-
315 ments carried out in the month of July, calibration line 1 was
316 used to obtain a reference moist airstream with a mixing
317 ratio of 15,000 ppmv, comparable to that of the analyzed
318 atmospheric air. In this case, two different reference waters
319 of known isotopic composition, named GS-90 and GS-91,
320 were stored in two tall (~1 m) and narrow columns with a
321 volume of 2 L. The large volume of the bubblers guarantees
322 that the isotopic composition change, due to the departure of
323 water from the column in the form of vapor, is completely
324 negligible. The isotopic composition of the GS-90 and
325 GS-91 reference waters was determined by repeated

IRMS analyses in our Groningen laboratory. The isotope 326
ratios are $\delta^2H = (-42.9 \pm 0.6)$‰ and $\delta^{18}O = (-6.34 \pm 0.02)$‰ 327
for GS-90, and $\delta^2H = (-170.3 \pm 0.5)$‰ and $\delta^{18}O = (-22.37 \pm$ 328
0.02)‰ for GS-91. A flow of dry nitrogen (grade purity 329
5.0 UN 1066 nitrogen, water content <~1 ppmv), from a 330
high-pressure tank, was passed ("bubbled") through the 331
water after entering at the bottom of the column. The flow 332
rate through the water column was set at 150 mL/min. The 333
moist stream leaving the column, and subsequently diluted 334
with nitrogen from the same tank in order to arrive at total 335
water-vapor content similar to the analyzed air, was led 336
through the laser spectrometer. The dilution ratio was 337
determined by mass flowmeters, whereas the exact mixing 338
ratio in this case was determined by the temperature and the 339
gas pressure in the bubbler column. Using this scheme, the 340
isotope ratio of the moist air exiting the column is thus not 341
identical to the liquid water feed, but a fractionation factor 342
that depends on the water-vapor temperature must be taken 343
into account. The expected delta values for the GS-90 344
standard in the moist stream are −16.05‰ and −121.3‰ for 345
$\delta^{18}O$ and δ^2H, respectively, given the fractionation factors of 346
−9.71‰ and −78.4‰ for ^{18}O and ^2H, in that order, at a 347
temperature of 20°C [*Majoube*, 1971]. This is in good 348
agreement with the experimental values determined by 349
cryogenically collecting the GS-90 saturated water-vapor 350
sample at the top of the column and analyzing it by IRMS: 351
The reported isotope ratios in this case were (−16.37 ± 352
0.02)‰ for $\delta^{18}O$ and (−120.7 ± 0.4)‰ for δ^2H. The actual 353

isotopic composition during the calibration cycles was determined using fractionation factors corresponding to the measured temperature in the climatically controlled room.

[24] Gas line 2 was used for calibration of the spectrometer at a mixing ratio value of 4,500 ppmv during the January measurements when mixing ratios were typically <5000 ppmv. This independent calibration scheme also served as a check on the bubbler-generated, diluted calibration streams. It uses a nozzle injector (Microdrop GmbH) to inject water droplets of known size at a preset repetition frequency into a stream of dry nitrogen or synthetic air. A detailed description of this system is published elsewhere [Iannone et al., 2009a]. The measurements were calibrated by the introduction of two local water standards, in this case GS-48 and GS-50. The GS-48 standard has an isotopic composition of (-43.3 ± 0.3)‰ for δ^2H and (-6.52 ± 0.03)‰ for $\delta^{18}O$, while the GS-50 standard has a value of (-276.7 ± 0.3)‰ and (-35.01 ± 0.03)‰ for δ^2H and for $\delta^{18}O$, respectively. Two nozzle injectors were employed in order to switch more rapidly between the two water standards.

[25] Finally, a comparison was made between our online laser spectrometer and the cryogenic sampling technique developed at the Commissariat à l'Énergie Atomique in Paris (CEA). The CEA device uses a trap cooled with an alcohol and dry ice slush and collects larger quantities of water, thus requiring a substantially larger flow (~2 L/min) than the laser spectrometer. Therefore, inlet line 3, which carries the ambient air, was equipped with a Y split. One part (150 mL/min) was led to the laser spectrometer, while the remainder went to the cryogenic collection device.

[26] Water-vapor samples were collected between 17 and 23 July 2007. Air continuously circulated through glass vapor traps immersed in an alcohol bath. The alcohol was kept at −80°C by periodically adding liquid nitrogen or ice slush. Samples were collected during time intervals lasting between 10 and 13 h for a single sample.

[27] No more than a maximum of two samples per day could thus be collected (e.g., between 1300 and ~2200/ 2330 h and between 2330 and ~1000 h of the following day. The long sample time is due to the fact we wanted to collect 2–3 ml of water, a requirement for precise IRMS analyses at CEA. The calibration of the spectrometer using the bubblers was then performed in the time interval between 1000 and 1300 h and generally completed in less than 1.5 h.

[28] The water collected in the traps was quantitatively transferred to a small container by cryogenic vacuum distillation, within 12 h after collection. The collected water was successively analyzed for its isotope ratios on IRMS instrumentation at CEA. As an additional check, a small fraction of a number of samples was transferred to different vials and analyzed at the Centrum voor IsotopenOnderzoek (Groningen, Netherlands) with the IRMS capabilities of the biomedical laboratory (able to handle samples as small as 10 μL).

[29] Finally, during the intercomparison measurements, temperature and humidity sensors (Tinytag, TGP-4500) were mounted on the top of the building roof, close to our air intake, in order to have a continuous registration of these two atmospheric parameters. Furthermore, meteorological data were taken from the Royal Netherlands Meteorological Institute (KNMI) Web site (accessible at http://www.knmi.nl).

3. Results and Discussion

[30] Figure 2 shows an example of data of the ambient vapor isotope ratios for the period from 19 to 22 January 2007, in Groningen, Netherlands. Although the instrument has a time resolution of a few seconds (determined by the gas exchange rate), for these long time series we show one data point per 5 min. With an averaging time of 300 s, the measurement precision was determined to be 0.20‰ for $\delta^{18}O$ and 0.75‰ for δ^2H at a water mixing ratio of ~15,000 ppm. These values are comparable to those reported previously for this spectrometer [Iannone et al., 2009a, 2009b], despite the relatively high value of the NEA, which was determined to be approximately 10^{-9} cm^{-1} Hz$^{-0.5}$, whereas a more typical value for this OFCEAS spectrometer is 4×10^{-10} cm^{-1} Hz$^{-0.5}$ [Kerstel et al., 2006].

[31] For reasons of clarity, the calibration data are not shown in the graphs but the corresponding periods are clearly visible as gaps in the data record (~10% of the overall measurement time).

[32] In Figure 2a, the black line (top curve) represents the relative humidity measured in our meteorological station of Lutjewad (about 40 km to the northwest of Groningen), while the shaded line (bottom curve) shows the ambient temperature. Figure 2b shows the amount of atmospheric water detected by our infrared laser spectrometer. It is worth noting how the spectrometer water-vapor mixing ratio follows a pattern consistent with the relative humidity, in agreement with the observation of small and often correlated variations in the outside temperature. Still, weather during this period was very variable and the relative humidity (RH) reached a maximum value of 93% between 19 and 20 January (day 1 and day 2), with an amount of rain of 2 mm. Between 20 and 21 January (day 2 and 3), rainfall reached 10 mm. The minimum value of 40% RH occurred by the end of 22 January (day 4), during a snow event.

[33] Over this 4 day period of measurements, δ^2H and $\delta^{18}O$ values also exhibited a high degree of variability, attributed to the dynamic meteorological conditions. The isotope values of deuterium span a wide range from −90‰ to −150‰, while the full range of variability of oxygen-18 measurements lies between about −16‰ and −33‰. The $\delta^{17}O$ measurements are not shown here since they are not expected to provide further information beyond that given by $\delta^{18}O$ due to the very tight relation between $\delta^{17}O$ and $\delta^{18}O$ observed in all tropospheric water [see, e.g., Meijer and Li, 1998]. In fact, the ^{17}O anomaly for our data, defined as $\Delta^{17}O = \ln(1 + \delta^{17}O) - 0.528 \, \mathrm{Ln}(1 + \delta^{18}O)$, assumes an average value of −0.4‰, equal to zero within the standard deviation of 1.6‰.

[34] Continuous measurements of atmospheric water-vapor isotopes were also performed between 17 and 23 July 2007. At the time of recording the data, also 10 atmospheric water vapor samples were collected by a cryogenic sample method (see section 2.2). During the same period, time-integrated rainfall samples were collected and subsequently analyzed by mass spectrometry (see the discussion of Figure 4b here below). As before, the daily averaged weather conditions were taken from the KNMI Web site.
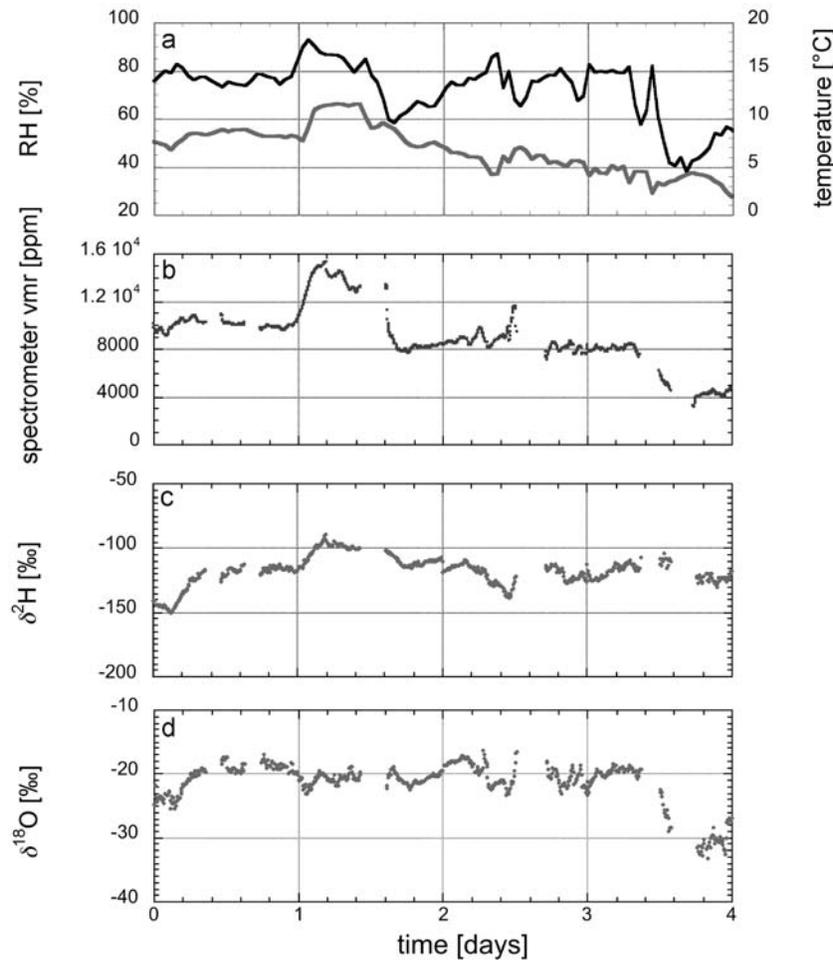
Figure 2. Continuous time series over 4 consecutive days with a 300 s time resolution: (a) ambient temperature and the simultaneously recorded relative humidity at the Lutjewad meteorological station (40 km NW of Groningen), (b) the volume mixing ratio of atmospheric air sampled from just outside the Groningen laboratory (53°N) as measured by the G2WIS spectrometer, (c) δ^2H, and (d) δ^{18}O. Two rain events and one snow event occurred during the 4 day measurement period (19–22 January). The horizontal arrows in Figure 2d indicate the precipitation events that occurred during these 4 days.

476 Figure 3a shows the 1-week time series of the relative
477 humidity and ambient temperature, and the spectrometer
478 water vapor content variation in the atmosphere, δ^2H, and
479 δ^{18}O are shown in Figures 3b, 3c, and 3d, respectively. For
480 clarity of presentation, the precipitation data are not shown.
481 Over this week, there was considerable variability in the
482 isotope ratios of δ^2H and δ^{18}O. The maximum values of δ^2H
483 and δ^{18}O were about −79‰ and −7.0‰, respectively, and
484 the minimum values were −135‰ and −23‰, respectively.
485 [35] In Figure 3 the horizontal bars represent the δ values
486 determined by the cryogenic trap described in section 2.2.
487 The extent of the bars corresponds to the sampling period.
488 [36] To be able to compare the results of the cold trap and
489 the laser spectrometer methods, mass-weighted average
490 δ^{18}O and δ^2H values are obtained by weighing the delta
491 values with the corresponding spectrometer water-vapor
492 mixing ratios. The summation is over all delta values
493 determined within the time frame of the cryogenic collection
494 in question. The data are reported in Table 1. We notice
495 that the overall deviation, given by the mean value of the

residuals, is −1.3‰ (1.7‰) for δ^{18}O and +1.0‰ (7.7‰) for 496
δ^2H, where the values in parentheses give the standard 497
deviation ($n = 10$). No clear correlation is observed between 498
the residuals of ^{18}O and ^{2}H. Similar differences between the 499
isotope ratio measurements obtained by means of laser and 500
those obtained by cryogenic collection and subsequent IRMS 501
analysis have been reported previously by other authors. 502
First, *Lee et al.* [2005] found an average difference of 503
−1.77‰ (1.75‰) for their ^{18}O measurements. This differ- 504
ence reduced to −0.36‰ (1.43‰) after correcting the data 505
for incomplete cryogenic collection. Later, *Wen et al.* [2008] 506
observed a disagreement between their TDL and cryogenic 507
sampling techniques of up to −10.4‰ and +4.9‰ for deu- 508
terium and oxygen-18, respectively. Also, no correlation 509
among the residuals of δ^2H and δ^{18}O could be seen [*Wen et* 510
al., 2008]. The authors attributed these differences to the 511
difficulties of condensing out all sample water vapor passing 512
through the cryogenic traps, as well as a combination of 513
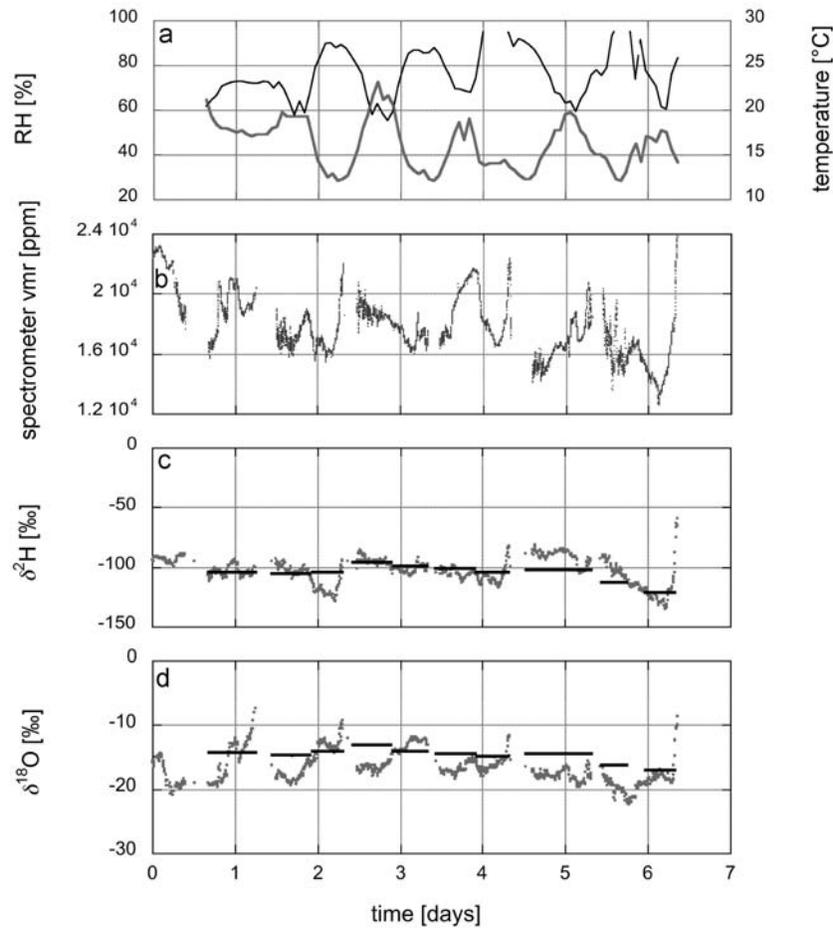errors in both the laser spectrometer and IRMS analyses. 514

Figure 3. Time series of 300 s isotope composition of ambient water vapor measured with the laser spectrometer during the week of intercomparison with the cold-trap method (17–23 July 2007): (a) ambient temperature and the simultaneously recorded relative humidity just outside the Groningen laboratory (53°N, 6°E), (b) volume mixing ratio of atmospheric air as measured by the G2WIS spectrometer, (c) δ^2H, and (d) the δ^{18}O. The horizontal bars give the δ^2H and δ^{18}O values determined by the water-vapor cryogenic sampling system, with the horizontal extent of the bars indicating the sampling period.

[37] In our case, the discrepancy is most likely caused by condensation and the subsequent evaporation within the ambient air gas-inlet line. In particular, during the early morning hours the air temperature can drop below the dewpoint temperature, causing a phase change within the sampling stream and consequently altering the vapor isotope content. Although an attempt was made to heat the tubing line during the measurements, this failed to heat the total

Table 1. Comparison of the Water Vapor Mixing Ratio-Weighted δ^2H and δ^{18}O Values of the Atmospheric Water Vapor as Measured by G2WIS, and by Cryogenic Collection Followed by IRMS Analysis, for the Data Shown in Figure 3 (Collected from 17 to 23 July 2007)[a]

Samples	δ^2H$_{IRMS}$ (‰)	δ^2_{LS} (‰)	Δ^2H$_{LS-IRMS}$ (‰)	δ^{18}O$_{IRMS}$ (‰)	δ^{18}O$_{LS}$ (‰)	Δ^{18}O$_{LS-IRMS}$ (‰)	υ_{H2O} (ppm)
1	−104.2	−102.9 (4.6)	−1.3	−14.3	−14.9 (3.3)	0.6	19098
2	−105.7	−104.5 (4.5)	−1.2	−14.8	−17.2 (1.2)	2.4	17449
3	−104.5	−117.9 (7.5)	13.4	−14.2	−13.0 (1.5)	−1.2	17300
4	−95.8	−96.1 (3.8)	0.3	−13	−16.1 (1.0)	3.1	18164
5	−99.9	−102.1 (3.3)	2.7	−14.1	−12.7 (0.9)	−1.4	17108
6	−101.3	−104.9 (3.4)	3.6	−14.5	−16.6 (0.9)	2.1	19786
7	−104.8	−107.6 (8.0)	2.8	−15	−16.1 (1.3)	1.1	18543
8	−102.6	−91.4 (6.1)	−11.2	−14.5	−17.9 (0.8)	3.4	16671
9	−112.9	−99.3 (6.0)	−13.6	−16.2	−19.2 (1.0)	3.0	16907
10	−121.9	−116.3 (13.7)	−5.6	−17	−17.3 (2.3)	0.3	15962
	Mean		1.00			−1.3	
	Standard deviation		7.8			1.7	
	Standard error		2.4			0.55	

[a]The standard deviations are given in parentheses. IRMS, isotope ratio mass spectrometry; LS, laser spectrometer.
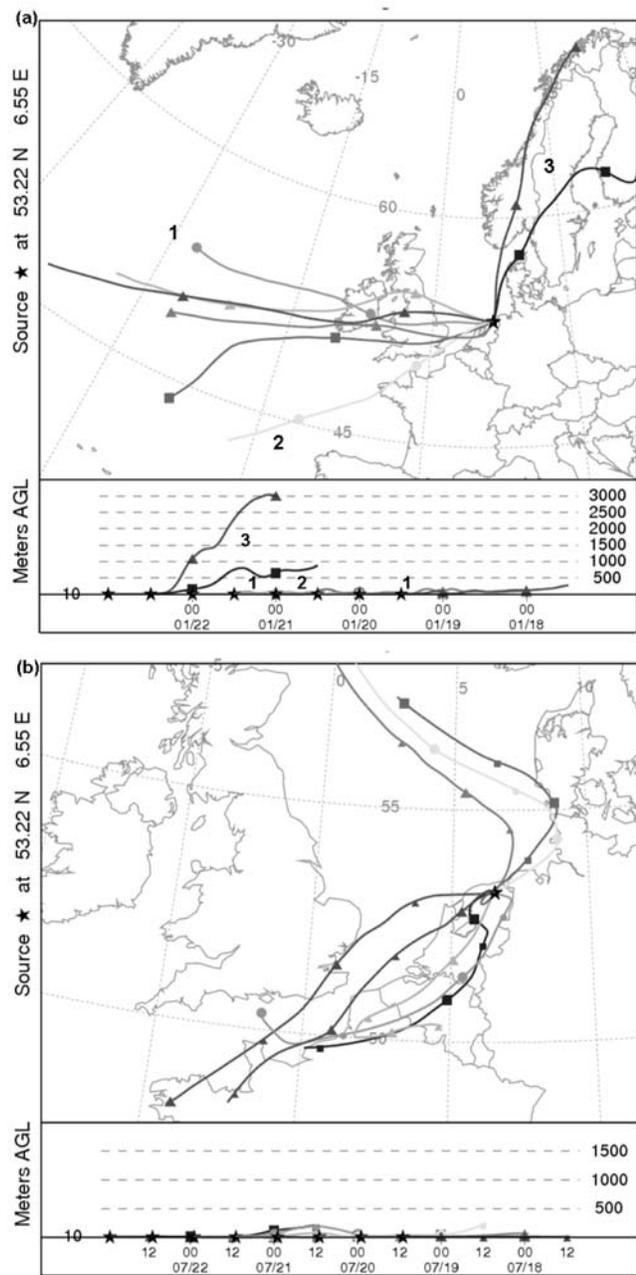
Figure 4. Twenty-four-hour-long backward trajectories produced by the NOAA HYSPLIT model. Two trajectories were calculated per day, one ending at 1200 and the other at 2400, for the two measurement periods: (a) 19–22 January and (b) 17–23 July 2007. Individual trajectories can be identified by their end time as is done in the bottom of each of Figures 4a and 4b. Trajectories start at 10 m above the ground. The boundary layer extended from 10 to 3000 m and from 10 to 1500 m for the months of January and July, respectively.

523 length of the inlet tube to temperatures above the high
524 summertime temperatures registered on some of the days.
525 The condensation of water vapor inside the inlet line is
526 particularly apparent in Figure 3 during the early morning
527 hours of days 2, 3, 5, and 7 by a rapid increase in the

528 measured mixing ratio beyond that predicted by the relative
529 humidity and temperature records, and sharply increasing
530 isotope ratio signals (especially visible in the [18]O record).
531 We believe that these excursions are due to the fact that the
532 liquid water, which formed earlier in the gas line during
533 periods of high outside temperatures, starts to evaporate
534 faster when the atmospheric water content decreases during
535 periods that combine a low outside temperature with a low
536 RH. Since, in all cases, these periods of excessively high
537 observed values of the volume mixing ratio are followed
538 immediately by a calibration cycle of the spectrometer, the
539 instrument is, as it were, reset. The flushing of the spec-
540 trometer with dry air, as part of the calibration cycle,
541 effectively removes the excess humidity in the inlet line.
542 The remainder of the data set is therefore believed to be still
543 largely representative of outside atmospheric moisture.

544 [38] When comparing the data between January and July,
545 a first difference to highlight concerns the variations in the
546 RH. During most of the days in the winter period the water
547 vapor content is fairly constant, whereas consistently higher
548 water-vapor mixing ratios are observed during daytime than
549 during nighttime in the summer season. This clear diurnal
550 variation is not observed in the January data, in agreement
551 with a strong diurnal temperature signal during the sum-
552 mertime measurements, which is absent in the winter data
553 set.

554 [39] It is noteworthy, however, that also during the winter
555 experiment, the RH reached high values (on one occasion as
556 high as 93%), and the absence of a diurnal cycle in this case
557 can be explained by large-scale transport and mixing of air
558 masses rather than the local meteorological conditions. This
559 interpretation of the data finds its origin in Figures 4a and
560 4b, which show backward trajectories computed using the
561 NOAA Hybrid Single Particle Lagrangian Integrated Tra-
562 jectory (HYSPLIT) model (available at http://www.arl.noaa.
563 gov/HYSPLIT.php) [*Draxler*, 1992; *Draxler and Hess*,
564 1998]. The figures show that, during winter, air originates
565 from both the western and southern Atlantic Ocean (area 1
566 and 2, respectively), as well as on some occasions from land
567 regions in Norway (area 3). During summer, although the
568 origin of air masses is variable, the direction of the majority
569 of the back trajectories is toward the south.

570 [40] The variations of the deuterium and oxygen-18 isotope
571 ratios in the atmospheric moisture are shown in Figures 5a
572 and 5b, which show δ^2H versus δ^{18}O for the January and
573 July measurements, respectively. In Figure 5, the global
574 meteoric waterline (GMWL) is shown together with an
575 evaporated waterline, with a slope of 4.5, intended here as a
576 point of reference for the measured isotope ratios.

577 [41] The GMWL describes the globally averaged stable
578 isotope composition of precipitation. During the evaporation
579 of meteoric water, relative humidity is the major factor
580 determining the isotopic composition of the atmospheric
581 vapor besides temperature and wind speed. Humidity affects
582 oxygen and hydrogen differently, such that the slope of the
583 evaporation line varies due to changes in water-vapor
584 mixing ratio content. This occurs because evaporation is
585 partly a nonequilibrium process and, particularly, because
586 lower relative humidity leads to a faster rate of evaporation
587 and, consequently, the kinetic fractionation will be greater.

588 [42] From Figure 5a, it is clear that the individual δ values
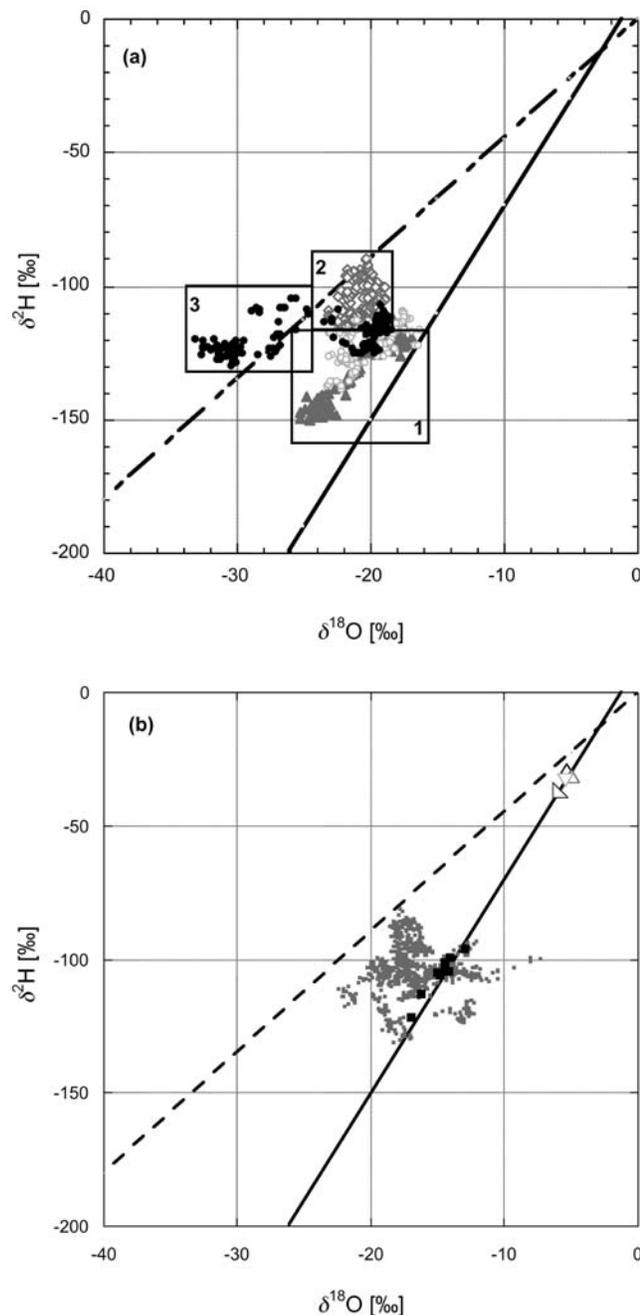589 of ^{2}H and [18]O are located slightly above the GMWL. The

Figure 5. The meteoric relationship for ^{18}O and ^{2}H in water vapor (a) between 19 and 22 January 2007 (19 January 2007, solid triangles; 20 January 2007, open diamonds; 21 January 2007, open circles; 22 January 2007, solid circles) and (b) between 17 and 23 July 2007. In Figure 5a the three rectangular shapes indicate three different groups of data, each corresponding to a different humidity ranges (40%–60%, area 3; 60%–80%, area 2; and finally 80%–100%, area 1). Data suspected of condensation in the gas line are excluded from Figure 5b. Furthermore, in Figure 5b, the open triangles represent the isotopic composition of the rain events of this week, whereas the solid squares give the isotopic composition of the atmospheric samples collected by the cryogenic sampling system. For comparison, the GMWL (continuous line) and the evaporated water line (dashed line) are shown.

isotope measurements are identified by day: 19 January 2007 (solid triangles), 20 January 2007 (open diamonds), 21 January 2007 (open circles), and 22 January 2007 (solid circles). Three different groups of data can be identified, each corresponding to a different source area, which becomes apparent when the data are correlated with the back trajectories of Figure 4a. In fact, on 19 and 21 January, the air masses are originating from the western Atlantic Ocean (area 1); on 20 January, the back trajectory has its origin over the southern Atlantic Ocean (area 2); whereas on 22 January, the air comes from Scandinavia (area 3). The different source regions of the air masses are also reflected in the local RH level, which is clearly not determined by the local temperature only (cf. Figure 2, top). In fact, the three different areas correspond to three RH ranges: from 40% to 60% (area 3), from 60% to 80% (area 2), and finally from 80% to 100% (area 1). The plot of $\delta^{18}O$ versus $\delta^{2}H$ yielded a significant ($r = 0.92$) straight-line relationship for the data of area 1. As well, the linear regression equation for the data of the second area shows a positive correlation ($r = 0.68$) between the $\delta^{18}O$ and $\delta^{2}H$ of the water vapor. Finally, a similar but slightly lower correlation ($r = 0.56$) is observed between deuterium and oxygen-18 in the data belonging to the third area.

[43] Figure 5b shows, besides the measured atmospheric moisture $\delta^{18}O$ and $\delta^{2}H$ isotope ratios, the four collected rain samples (triangles). The solid squares represent instead the isotopic composition of the atmospheric water vapor measured by cryogenic collection and subsequent IRMS analysis. Both the laser spectrometer and the IRMS data lie significantly closer to the GMWL compared to the data of January. In particular, as for the laser spectrometer data, the IRMS data are also found above the GMWL. The best fit through the IRMS data defines a slope $\delta^{2}H/\delta^{18}O$ equal to 6.3 (±0.6). This is a consequence of the higher RH. During this summer week, the humidity level reached values of about 96% in a strong diurnal cycle, and rain events occurred during the night from 17 to 18 July, and on 20, 21, and 22 July. These precipitation events are the main cause of variation of $\delta^{18}O$ and $\delta^{2}H$. Precipitation leads to a more negative isotopic composition of the remaining vapor, while the increased humidity reduces the evaporation of local surface water. Moreover, rain events are generally linked to the arrival of different (warmer) air masses.

[44] It should be noted that the laser spectrometer isotope data show significantly higher variation than the cryogenically collected samples. This is mostly due to the fact that the cryogenic collection method suffers from a strong bias toward high water content periods, especially given the extremely long sample collection times that were required to collect an amount of liquid water sufficiently large for isotopic analysis at the CEA laboratory in Paris.

[45] Figures 5a and 5b are thus in good agreement with theoretical considerations according to which high levels of humidity result in a better isotope equilibrium between liquid and vapor and a MWL with a slope closer to 8 [*Clark and Fritz*, 1997].

[46] In addition, it is possible to observe the influence of air originating from land regions in Scandinavia on the isotopic signature during the week in January. In particular, the arrival of these relatively dry air masses from northwesterly regions results in strong changes in the $\delta^{18}O$ of
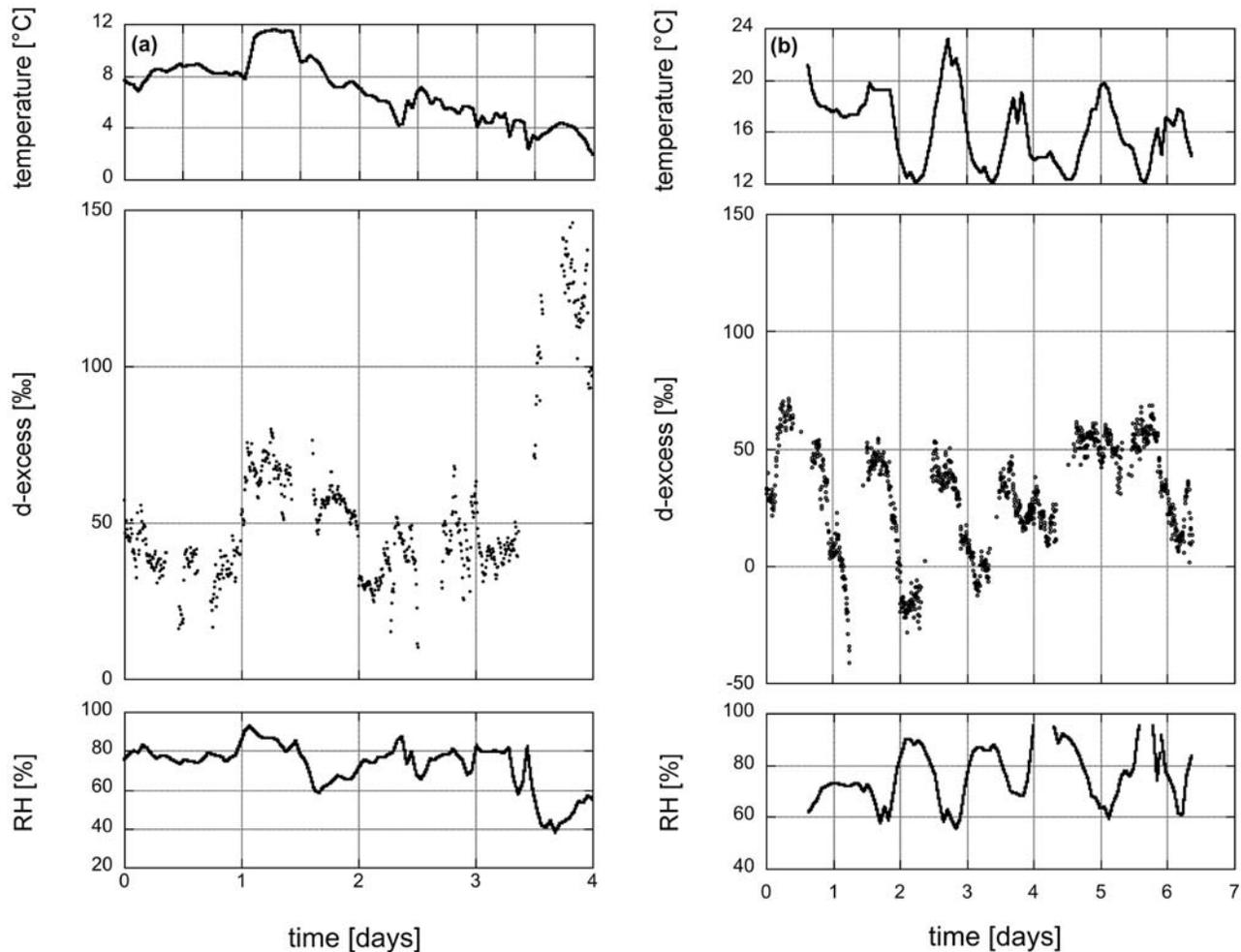
Figure 6. Time series of *d* excess based on the laser spectrometry method for (a) 19–22 January and (b) 17–23 July 2007: (top) ambient temperature and (bottom) relative humidity.

652 atmospheric water vapor. In fact, data of the second half of
653 the day on 22 January (Figure 5a) have δ^{18}O values that are
654 consistently far from the GMWL. As a matter of fact, this
655 necessarily indicates that isotope fractionation in the
656 hydrologic cycle during this part of the day is not governed
657 by liquid-vapor equilibrium. *Jouzel and Merlivat* [1984]
658 proposed that nonequilibrium condensation becomes sig-
659 nificant when sublimation on ice crystals occurs. These data,
660 in fact, come from a period of a cold front passage during
661 which snowfall occurred, corresponding to a sharp
662 decreasing of the humidity as shown in Figures 2 (top) and 4a.
663 This snow event explains why δ^{18}O is so much lower com-
664 pared to the previous period.

665 [47] During these particular meteorological conditions, the
666 decrease in the δ^2H value is less remarkable than that for
667 ^{18}O. This can be explained in terms of higher deuterium
668 excess, defined as $d = \delta^2$H-8 · δ^{18}O [*Dansgaard*, 1964], due
669 to a strong kinetic evaporation, which takes place into
670 unsaturated air. Vapor generated under low-humidity con-
671 ditions has a high deuterium excess, as a result of the fact
672 that the relative contribution of kinetic fractionation is larger
673 for ^{18}O than for ^{2}H [*Araguás Araguás et al.*, 2000]. This is
674 very visible in Figure 6a, where the deuterium excess, for
675 the January week, is graphed with the ambient temperature

and the RH. Typical values of *d* excess in rain samples in 676
the Groningen region vary between 10‰ and 30‰. In our 677
case, since the data define a δ^2H/δ^{18}O slope <8, the *d* excess 678
shows higher values. During the week in January, the deu- 679
terium excess ranged between +20‰ and +75‰ for most of 680
the measurements period, except for the second half of the 681
last day (22 January), where *d* excess reached values up to 682
+125‰, indicating extreme low-moisture conditions. High 683
values of *d* excess were also found by *Angert et al.* [2008]. 684
In their publication they discuss results of measurements of 685
the isotopic composition of atmospheric water vapor per- 686
formed over 9 years (1998–2006). Although the temporal 687
resolution is not very high, they report *d* excess values up to 688
+50‰ during wintertime. The measurements were carried 689
out in Israel, at which latitude one would normally expect to 690
see lower deuterium excess values than at the higher latitude 691
of our study. More important, the cryogenic collection 692
method of the Israeli study is strongly biased toward high 693
humidity (since during periods of high humidity more water 694
is collected than during equally long low-humidity periods) 695
and, thus, low deuterium excess, exacerbated by the long 696
data collection times. From Figure 6a, we thus conclude that 697
the *d* excess increases as the RH under which the evapo- 698
ration occurred decreases. A plot of the *d* excess versus the 699

local RH shows a statistically significant correlation ($r = 0.60$) under dry winter conditions. In addition, air masses with different moisture characteristics, due to their different origins, have higher d excess values and the d excess value can provide specific information to identify the mixing of evaporated air in the atmosphere.

[48] Figure 6b shows d excess for the week in July compared with temperature and humidity. During these summertime measurements, the d excess was negatively correlated with the RH with a correlation coefficient of 0.48. If the humidity is low, d excess values are high. In contrast, d excess values corresponding to high humidity are low. Again we see that the d excess may give insight into the RH deficit in air masses.

[49] These observations are in good agreement with the work of *Uemura et al.* [2008], who determined deuterium excess of atmospheric water vapor above the Southern Ocean in order to provide detailed knowledge of ocean surface conditions.

4. Conclusion

[50] We have applied our instrument, originally designed for the in situ isotope analysis of stratospheric water vapor, to continuous, ground-based atmospheric water-vapor isotope measurements.

[51] Two approximately 1 week long data sets were recorded, one in January and the other in July 2007. The July data set was compared to IRMS analyses on moisture samples collected simultaneously by a cryogenic technique. Differences between the two different measurement strategies are attributed to condensation in the inlet line that affects mostly the laser measurements, as well as to incomplete sample collection in case of the cryogenic method. Thanks to the high time resolution of the laser method, as well as its continuous measurement nature, the inline condensation events are easily identified in both the volume mixing ratio and the isotope ratio records. The data sets also make it very apparent that the cryogenic technique is strongly biased toward high-water-concentration data and thus misses many of the most interesting features at low-water-volume mixing ratios visible in the continuous, high-resolution record.

[52] A strong positive relationship is observed between the isotopic composition of the water vapor and its mixing ratio, suggesting that the RH is the main meteorological parameter controlling the isotope distribution near the surface, as has been demonstrated previously in other related studies [*Angert et al.*, 2008; *Jacob and Sonntag*, 1991; *White and Gedzelman*, 1984].

[53] Even with the relatively small data set of this study, interesting differences between the behavior of the isotope signals in the winter and summer seasons are apparent. In particular, we observe that in summer the evaporation and the precipitation processes affect both deuterium and oxygen-18 simultaneously. High temperatures and high levels of humidity result in a near-isotopic equilibrium between air moisture and precipitation. Furthermore, the summer data show a clear diurnal cycle, in contrast to the winter data. In the wintertime, on the contrary, the interaction of fresh dry air from northwest of Groningen with western Atlantic Ocean air masses makes the change in the deuterium and oxygen-18 isotopes decoupled to a larger extent than is the case in the summer season. For this reason also, the atmospheric moisture shows a large deuterium excess in winter.

[54] Nowadays, measurements of water vapor isotopes have become a significant topic in several fields of research, for example, in hydrology and ecology. With the introduction of laser technology, it has become increasingly possible to perform simultaneous in situ measurements of δ^2H and δ^{18}O in water vapor, making the optical isotope ratio technique definitely competitive with IRMS. Water-vapor isotope samples obtained with a cryogenic system, and subsequently analyzed with IRMS, can provide only an episodic picture of the weather conditions, which may turn out to be insufficient for reliable conclusions concerning changes in atmospheric water vapor.

[55] So far, the calibration of a laser spectrometer to measure water-vapor isotopes in near-surface atmospheric air has been most commonly done by means of a dew point generator [*Lee et al.*, 2005; *Wen et al.*, 2008]. This requires the knowledge of temperature-dependent isotope fractionation factors since the isotopic composition of the vapor is related to that of the liquid in the reservoir, and the need of relatively large quantities of water involved makes this procedure relatively expensive and quite unsuitable for field applications. The microdrop method developed by us can be easily extended to higher volume mixing ratios and is likely to become an important alternative to the dew point generator [*Iannone et al.*, 2009a]. The problems encountered with condensation in the inlet tubing during the summertime measurements in this preliminary study are easily resolved by properly heating the entire length of the inlet tube (e.g., by Ohmic heating) or by reducing the pressure in the inlet tube immediately after the air intake.

[56] Monitoring the stable isotope composition of atmospheric water vapor can provide a continuous record of valuable data on the atmospheric hydrological cycle. This will help to further understand the functioning of, and interactions between, the water cycle and other biogeochemical cycles, which in combination with retrieved observations by satellites will enable global mapping of the water cycle.

References

Angert, A., J.-E. Lee, and D. Yakir (2008), Seasonal variations in the isotopic composition of near-surface water vapour in the eastern Mediterranean, *Tellus*, doi:10.1111/j.1600-0889.2008.00357.

Araguas Araguas, L., P. Danesi, K. Froehlich, and K. Rozanski (1996), Global monitoring of the isotopic composition of precipitation, *J. Radioanal. Nucl. Chem.*, 205, 189–200, doi:10.1007/BF02039404.

Araguás-Araguás, L., K. Froehlich, and K. Rozanski (2000), Deuterium and oxygen-18 isotope composition of precipitation and atmospheric moisture, *Hydrol. Process.*, 14, 1341–1355, doi:10.1002/1099-1085(20000615) 14:8<1341::AID-HYP983>3.0.CO;2-Z.

Barkan, E., and B. Luz (2007), Diffusivity fractionations of (H$_2$O)-O-16/ (H$_2$O)-O-17 and (H$_2$O)-O-16/(H$_2$O)-O-18 in air and their implications for isotope hydrology, *Rapid Commun. Mass Spectrom.*, 21(18), 2999–3005, doi:10.1002/rcm.3180.

Clark, I. D., and P. Fritz (1997), *Environmental Isotopes in Hydrogeology*, CRC Press, Boca Raton, Fl.

Dansgaard, W. (1964), Stable isotopes in precipitation, *Tellus*, 16, 436–438, doi:10.1111/j.2153-3490.1964.tb00181.x.

823 Draxler, R. R. (1992), *Hybrid Single-Particle Lagrangian Integrated*
824 *Trajectories (HY-SPLIT): Version 3.0—User's Guide and Model*
825 *Description*, *Tech. Memo. ERL ARL-195*, p. 26 and Appendices. Envi-
826 ron. Res. Lab. (NOAA), Boulder, Colo.
827 Draxler, R. R., and G. D. Hess (1998), An overview of the HYSPLIT_4
828 modelling system for trajectories, dispersion and deposition, *Aust.*
829 *Meteorol. Mag.*, *47*, 295–308.
830 Galewsky, J., D. Noone, Z. Sharp, and J. Woerden (2009), Water vapor
831 isotopes measurements at Mauna Loa, Hawaii: Comparison of laser
832 spectroscopy and remote sensing with traditional methods, and the need
833 for ongoing monitoring, paper presented at European Geosciences
834 Union General Assembly 2009, Vienna, 19–24 April.
835 Gonfiantini, R. (1978), Standards for stable isotope measurements in
836 natural compounds, *Nature*, *271*, 534–536, doi:10.1038/271534a0.
837 Gonfiantini, R. (1984), Report of the advisory group meeting on stable iso-
838 tope reference samples for geochemical and hydrological investigations,
839 Int. At. Energy Agency, Vienna.
840 Griffith, D. W. T., I. Jamie, M. Esler, S. R. Wilson, S. D. Parkes, C. Waring,
841 and G. W. Bryant (2006), Real-time field measurements of stable isotopes
842 in water and CO_2 by Fourier transform infrared spectrometry, *Isotopes*
843 *Environ. Health Stud.*, *42*, 9–20, doi:10.1080/10256010500503098.
844 He, H., and R. B. Smith (1999), Deuterium in water vapor evaporated from
845 a coastal salt marsh, *J. Geophys. Res.*, *104*(D9), 11,675–11,673,
846 doi:10.1029/1998JD100108.
847 Hut, G. (1987), Report to the director general, Int. At. Energy Agency,
848 Vienna.
849 Iannone, R. Q., D. Romanini, S. Kassi, H. A. J. Meijer, and E. R. Th. Kerstel
850 (2009a), A microdrop generator for the calibration of a water vapor iso-
851 tope ratio spectrometer, *J. Atmos. Oceanic Technol.*, *26*, 1275–1288,
852 doi:10.1175/2008JTECHA1218.1.
853 Iannone, R. Q., S. Kassi, M. Chenevier, H.-J. Jost, D. Romanini, H. A. J.
854 Meijer, and E. R. T. Kerstel (2009b), Development and airborne opera-
855 tion of a compact water isotope ratio infrared spectrometer, *Isotopes*
856 *Environ. Health Stud.*, *45*, 303–320, doi:10.1080/10256010903172715.
857 Jacob, H., and C. Sonntag (1991), An 8-year record of the seasonal varia-
858 tion of ^2H and ^{18}O in atmospheric water vapor and precipitation at Hei-
859 delberg, Germany, *Tellus*, *43B*, 291–300.
860 Jouzel, J., and L. Merlivat (1984), Deuterium and oxygen 18 in precipita-
861 tion: Modeling of the isotopic effects during snow formation, *J. Geophys.*
862 *Res.*, *89*(D7), 11,749–11,757, doi:10.1029/JD089iD07p11749.
863 Kerstel, E., and L. Gianfrani (2008), Advances in laser-based isotope ratio
864 measurements: Selected applications, *Appl. Phys. B*, *92*(3), 439–449,
865 doi:10.1007/s00340-008-3128-x.
866 Kerstel, E. R. T. (2004), Isotope ratio infrared spectrometry, in *Handbook*
867 *of Stable Isotope Analytical Techniques*, edited by P. A. de Groot, chap.
868 34, pp. 759–787, Elsevier, Amsterdam.
869 Kerstel, E. R. T., R. Q. Iannone, M. Chenevier, S. Kassi, H.-J. Jost, and
870 D. Romanini (2006), A water isotope (^2H, ^{17}O, and ^{18}O) spectrometer

871 based on optical-feedback cavity enhanced absorption for *in situ* air-
872 borne applications, *Appl. Phys. B*, *85*(2–3), 397–406, doi:10.1007/
873 s00340-006-2356-1.
874 Lee, X., S. Sargent, R. Smith, and B. Tanner (2005) In situ measurement
875 of the water vapor $^{18}O/^{16}O$ isotope ratio for atmospheric and ecological
876 applications, *J. Atmos. Oceanic Technol.*, *22*, 555–565, doi:10.1175/
877 JTECH1719.1.
878 Majoube, M. (1971), Fractionnement en oxygène-18 et en deutérium entre
879 l'eau et sa vapeur, *J. Chem. Phys.*, *197*, 1423–1436.
880 Meijer, H., and W. Li (1998), The use of electrolysis for accurate ^{17}O and
881 ^{18}O isotope measurements in water isotopes, *Isotopes Environ. Health*
882 *Stud.*, *34*, 349–369, doi:10.1080/10256019808234072.
883 Morville, J., S. Kassi, M. Chenevier, and D. Romanini (2005), Fast, low-
884 noise, mode-by-mode, cavity-enhanced absorption spectroscopy by
885 diode-laser self-locking, *Appl. Phys. B*, *80*, 1027–1038, doi:10.1007/
886 s00340-005-1828-z.
887 Rothman, L. S., et al. (2005), The HITRAN molecular spectroscopic data-
888 base, *J. Quant. Spectrosc. Radiat. Transf.*, *96*, 139–204, doi:10.1016/j.
889 jqsrt.2004.10.008.
890 Uemura, R., Y. Matsui, K. Yoshimura, H. Motoyama, and N. Yoshida
891 (2008), Evidence of deuterium excess in water vapor as an indicator of
892 ocean surface conditions, *J. Geophys. Res.*, *113*, D19114, doi:10.1029/
893 2008JD010209.
894 Wang, L., K. K. Caylor, and D. Dragoni (2009), On the calibration of con-
895 tinuous, high-precision $\delta^{18}O$ and δ^2H measurements using an off-axis
896 integrated cavity output spectrometer, *Rapid Commun. Mass Spectrom.*,
897 *23*, 530–536, doi:10.1002/rcm.3905.
898 Wang, X. F., and D. Yakir (2000), Using stable isotopes of water in evapo-
899 transpiration studies, *Hydrol. Process.*, *14*(8), 1407–1421, doi:10.1002/
900 1099-1085(20000615)14:8<1407::AID-HYP992>3.0.CO;2-K.
901 Wen, X.-F., X.-M. Sun, S.-C. Zhang, G.-R. Yu, S. D. Sargent, and X. Lee
902 (2008), Continuous measurement of water vapor D/H and $^{18}O/^{16}O$ iso-
903 tope ratios in the atmosphere, *J. Hydrol. Amsterdam*, *349*, 489–500,
904 doi:10.1016/j.jhydrol.2007.11.021.
905 White, J. W. C., and S. D. Gedzelman (1984), The isotopic composition
906 of atmospheric water vapor and the concurrent meteorological conditions,
907 *J. Geophys. Res.*, *89*(D3), 4937–4939, doi:10.1029/JD089iD03p04937.
908 Worden, J. R., et al. (2007), Importance of rain evaporation and continental
909 convection in the tropical water cycle, *Nature*, *445*, 528–532,
910 doi:10.1038/nature05508.

911 O. Cattani, LSCE, IPSL CEA Saclay, 91191 Gif sur Yvette, France.
912 R. Q. Iannone, E. R. Th. Kerstel, and H. A. J. Meijer, Centrum voor
913 IsotopenOnderzoek, University of Groningen, NL-9747 AG Groningen,
914 Netherlands. (e.r.t.kerstel@rug.nl)
915 D. Romanini, Laboratoire de Spectrométrie Physique, UMR 5588,
916 Université J. Fourier Grenoble, CNRS, 38402 Saint Martin d'Hères, France.